

International Conference on Space Optics—ICSO 2014

La Caleta, Tenerife, Canary Islands

7–10 October 2014

Edited by Zoran Sodnik, Bruno Cugny, and Nikos Karafolas



Selection of fiber-optical components for temperature measurement for satellite applications

P. Putzer

N. Kuhenuri Chami

A. W. Koch

A. Hurni

et al.



International Conference on Space Optics — ICSO 2014, edited by Zoran Sodnik, Nikos Karafolas, Bruno Cugny, Proc. of SPIE Vol. 10563, 105631C · © 2014 ESA and CNES
CCC code: 0277-786X/17/\$18 · doi: 10.1117/12.2304276

SELECTION OF FIBER-OPTICAL COMPONENTS FOR TEMPERATURE MEASUREMENT FOR SATELLITE APPLICATIONS

P. Putzer¹, N. Kuhenuri Chami¹, A. W. Koch¹, A. Hurni², M. Roner², J. Obermaier², N. M.K. Lemke²
¹*Technische Universität München, Lehrstuhl für Messsystem- und Sensortechnik, 80333 Munich, Germany, p.putzer@tum.de*
²*OHB System AG, Wolfratshauser Straße 48, 81379 Munich, Germany, andreas.hurni@ohb.de.*

I. ABSTRACT

The Hybrid Sensor Bus (HSB) is a modular system for housekeeping measurements for space applications. The focus here is the fiber-optical module and the used fiber-Bragg gratings (FBGs) for temperature measurements at up to 100 measuring points. The fiber-optical module uses a tunable diode laser to scan through the wavelength spectrum and a passive optical network for reading back the reflections from the FBG sensors. The sensors are based on FBGs which show a temperature dependent shift in wavelength, allowing a high accuracy of measurement.

The temperature at each sensor is derived from the sensors Bragg wavelength shift by evaluating the measured spectrum with an FBG peak detection algorithm and by computing the corresponding temperature difference with regard to the calibration value. It is crucial to eliminate unwanted influence on the measurement accuracy through FBG wavelength shifts caused by other reasons than the temperature change. The paper presents gamma radiation test results up to 25 Mrad for standard UV-written FBGs in a bare fiber and in a mechanically housed version. This high total ionizing dose (TID) load comes from a possible location of the fiber outside the satellite's housing, like e.g. on the panels or directly embedded into the satellites structure. Due to the high shift in wavelength of the standard written gratings also the femto-second infrared (fs-IR) writing technique is investigated in more detail.

Special focus is given to the deployed fibers for the external sensor network. These fibers have to be mechanically robust and the radiation induced attenuation must be low in order not to influence the system's performance. For this reason different fiber types have been considered and tested to high dose gamma radiation. Dedicated tests proved the absence of enhanced low dose rate sensitivity (ELDRS). Once the fiber has been finally selected, the fs-IR grating will be written to these fibers and the FBGs will be tested in order to investigate the radiation induced wavelength shift.

The FBGs react on temperature and strain change, so a decoupling of both physical effects must be assured to allow a precise measurement over large temperature ranges and corresponding potential mechanical stress, passed from the structure to the sensor. This potential source of error is addressed with the design of a strain-decoupled temperature transducer to which the FBGs are glued. The design of the transducer and measurement results of a bending test are provided within this paper.

An outlook of the usage of fiber-optical sensing in space applications will be given. One promising field of application are the so called photonically-wired spacecraft panels, where optical fibers with integrated FBGs are being integrated in panels for temperature measurements and high-speed data transfer at the same time.

II. SCANNING LASER BASED INTERROGATOR

The interrogator module is based on a modulated grating Y-branch (MGY) tunable laser illustrated in detail in Fig. 1. The wavelength tuning of the laser in its spectral range spanning from 1528 nm to 1568 nm (C-band) is done over three input currents, namely the left and right reflector current and the phase current.

Inside the control FPGA (field-programmable gate array), a look-up table is stored wherein the relation between laser wavelengths and reflector currents is implemented. During a measurement cycle, the tunable laser scans through the full spectrum and the reflected light from the FBG array is measured by a photodiode. The reflected intensity signal is assigned to the output wavelength again in terms of a look-up table (LuT). Afterwards, the setup wavelength and the reflected signal are evaluated by the FPGA by means of dedicated algorithms. When the shift in Bragg wavelength is determined by the FPGA, the assignment to a physical temperature will be performed.

The measurement system can easily be adapted to more sensor strings by the implementation of additional photodiodes and passive optical couplers as long as the signal-to-noise-ratio (SNR) stays at an adequate level.

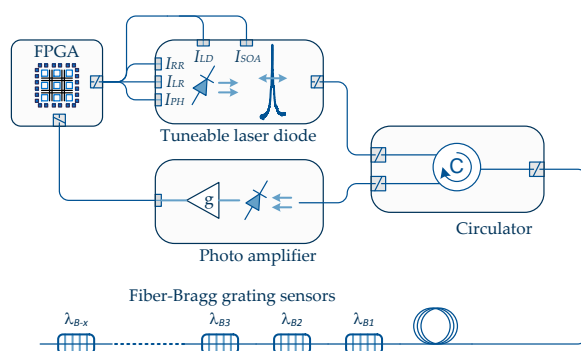


Fig. 1: Fiber-optic interrogator based on a tunable laser with control FPGA, optical circulator, fiber-Bragg grating sensors and photo amplifier (photodiode plus transimpedance amplifier).

III. FBG MEASUREMENT PRINCIPLE

As fiber-optical sensor the fiber-Bragg grating (FBG) sensor is used. This sensor allows measurements of temperature and/or strain without electrical signals. A grating structure with a modulated refractive index along the fiber axis is written by a UV-excimer laser (193 nm or 248 nm) in a photosensitive fiber [10, 11]. Another manufacturing process is the writing of the grating by femto-second infrared (fs-IR) pulses [12, 3, 9].

After the writing process a wavelength dependent band-stop filter is formed in the fiber whereof the Bragg-wavelength can be approximated to

$$\lambda_B = 2 \cdot n_{eff} \cdot \Lambda \tag{1}$$

where λ_B is the Bragg-wavelength, n_{eff} is the effective refractive index and Λ is the grating pitch. Only light corresponding to the Bragg-wavelength λ_B is reflected back to the light source, light outside the Bragg-wavelength can pass the FBG without any loss. This is illustrated in detail in Fig. 2.

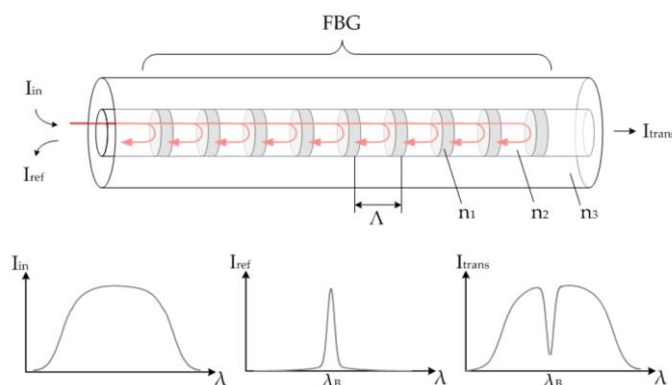


Fig. 2: FBG with pitch period Λ and reflected light (top). Bottom, left to right: A broadband optical light is coupled into the FBG, and only light with the Bragg-wavelength is reflected (middle). The transmitted light shows a dip at the wavelength position where the reflection occurs.

The fact that light which does not correspond to the Bragg-wavelength can pass the FBG sensor is used to build a multi-sensor wavelength-division multiplexing (WDM) system. In this way many sensors can be read out with a single interrogator module and no additional switching components. The Bragg-wavelength of each sensor in the fiber must differ from each other and must be adequately spaced in wavelength to avoid a mixing of the sensor responses due to strong differences in sensor temperatures. The principle of forming a WDM FBG sensor array is shown in Fig. 3.

The number of embedded FBGs is limited by the optical broadness of the illuminating light source and by the necessary spectral bandwidth of each sensor. The laser can be tuned within a bandwidth of 40 nm and by taking into account the fact that one sensor needs a bandwidth of approximately 4 nm to cover the full temperature range from -100°C to $+100^\circ\text{C}$, the maximum number of sensors per string is given to ten sensors.

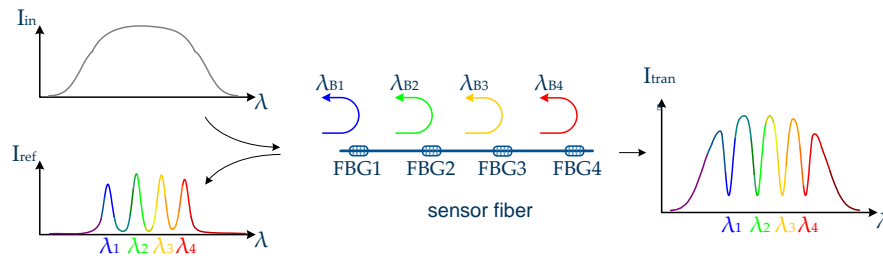


Fig. 3: FBG sensor array is illuminated with a broad light source (top left) and the transmission (right side) and reflection spectra (bottom left) are shown.

The shift in Bragg-wavelength according to equation (2) can be split up in two terms. The first term is affected by the applied strain to the sensor and the second term is affected by changes in sensor temperature. In silica fibers the change in the Bragg-wavelength is given per 95 % by the temperature dependent refractive index change dn/dT , whereas the change in the fiber length due to thermal expansion α amounts only to $\approx 5\%$.

The presented design uses a laser with a central wavelength at 1550 nm, so the shift from the initial Bragg-wavelength due to strain changes $\Delta\varepsilon$ and temperature changes ΔT can be computed to [10]:

$$\Delta\lambda_B [pm] = 1.209 \frac{pm}{\mu\varepsilon} \cdot \Delta\varepsilon + 10.338 \frac{pm}{K} \cdot \Delta T. \tag{2}$$

When the sensor is mounted on a strain insensitive platform on which only temperature changes affect the shift in the Bragg-wavelength, then a conclusion with respect to the temperature at the sensor location can be made. An appropriate transducer design is shown in the next section.

IV. TRANSDUCER DESIGN

As seen before the FBG sensor is written into an optical fiber, which is general very thin and lightweight but also very sensitive to mechanical forces like twist, stress and shear strains. In addition the shift in Bragg-wavelength depends on temperature and strain applied to the grating. In order to gain mechanical robustness and due to the necessity for strain decoupling a special transducer was designed. A 3D-model is given in Fig. 4. The size of the transducer is 8 mm x 20 mm with a thickness of 1.5mm. The fiber will only be glued onto the middle paddle of the transducer at the fiber position where the grating is located. On the side grooves (shown in the picture in Fig. 4 on the right) only the fiber protection tube is glued. So if the structure where the sensor is mounted is bent, the middle paddle is not affected by this force and the FBG's Bragg-wavelength stays constant for constant temperatures.

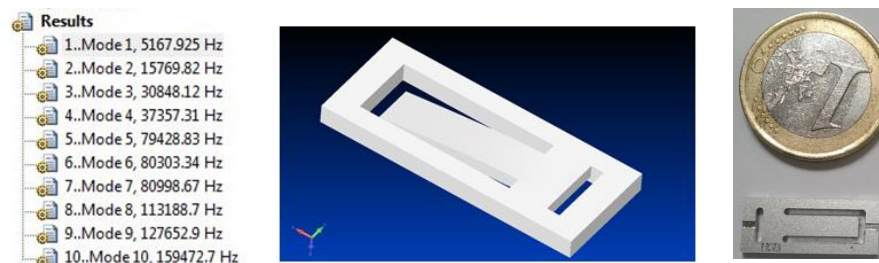


Fig. 4: 3D-model of the designed transducer with its Eigen frequencies (left) in the simulation with extreme values. Picture of the final transducer made out of aluminum with respect to the size of a One Euro coin (right).

The next step was to prove the concept of strain decoupling with the designed transducer. For this an FBG (FBG4) was glued onto the middle paddle and the complete transducer was glued on an aluminum plate. The reflected wavelength from the grating was measured during the plate was bent according to the four-point bending test. In addition to the transducer presented above two additional sensors were glued next to each other, FBG3 implemented in a PEEK hull with vacuum grease (experimental) and FBG5 glued directly onto the aluminum plate acting as reference.

The measurement result is given in Fig. 5 for all three sensors. The blue curve (bottom line) shows the result of the FBG sensor which is directly glued to the aluminium plate. The shift in Bragg-wavelength is quite high; a linear fit resulted in a value of 336.4 pm/mm. The shift of the designed transducer (red mark, middle line) is in

the range of 0.8 pm/mm which is a comparable good result. For the transducer mounted into the PEEK hull with the vacuum grease the shift in wavelength is even lower, the linear fit shows a change in Bragg-wavelength of 0.2 pm/mm. The sensitivity of the wavelength shift to temperature can be approximated to 10 pm/K, so also a 0.8 pm shift corresponds only to a temperature error of 0.08 K.

The measurement campaign has shown that the transducer design works pretty good and decouples the mechanical strain from the structure to the FBG sensor. The transducer where the FBG is mounted with the vacuum grease showed also good results, but the implementation of the grease and the thereby possible pollution of other components during assembly phase is seen as risky.

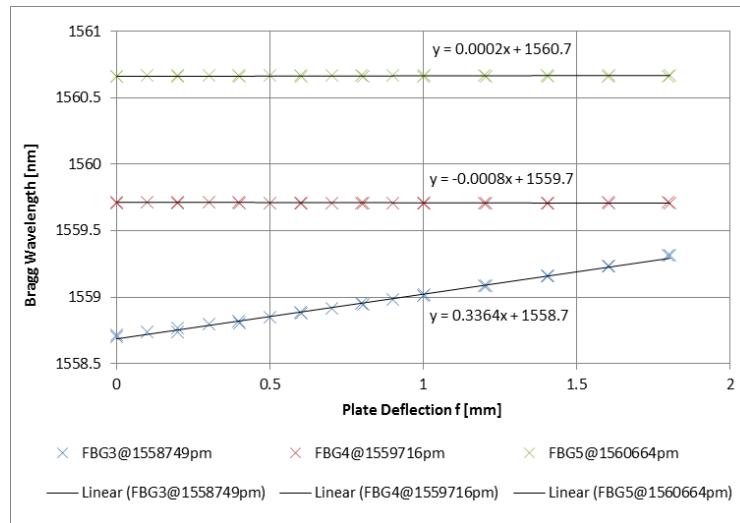


Fig. 5: Measurement results of the four-point bending test, FBG3 is the sensor glued directly on the plate, FBG4 is the designed transducer and FBG5 the experimental sensor implemented in the protection hull with vacuum grease.

Another important parameter of the transducer is the time constant. In the case here the time constant is defined as the time which is necessary to see 1 K temperature difference between middle paddle (sensor position) and outer frame (mounting interface). The simulation is carried out for aluminum (Al6061) and titan (Ti6Al4V), showing very high differences in time constants.

Material	Time Constant [sec.]			Equilibrium (99.7%) [sec]		
	Front	Mid	End	Front	Mid	End
Al6061	0.197	1.077	1.336	4.8	6.0	6.3
Ti6Al4V	4.40	23.9	29.7	106.5	133.6	139.7

Fig. 6: Simulation results for the time constant of the transducer made out of aluminum (Al6061) and titan (Ti6Al4V).

The notation “Front”, “Mid” and “End” denotes the position of the middle paddle where “End” is the point most far away from the cross brace. The time constants are approximately 22 times larger for titan than for aluminum. By using aluminum also the sensitivity of the sensor is changed to higher values because aluminum has a higher thermal expansion coefficient than titan and glass (SiO₂). When the temperature changes, the aluminium transducer is stretched. This can be seen by the FBG as an additional temperature dependent strain. This is not the case when titan is used. General speaking, a higher sensitivity is advantageous in most applications.

The simulated equilibrium temperature as function of time is shown in Fig. 7 for aluminium (left) and titan (right). For correct interpretation of the simulation the value of the Mid-point must be taken because this is the location where the grating is mounted. For the simulation only conductive heat transfer was used, no radiative transfer.

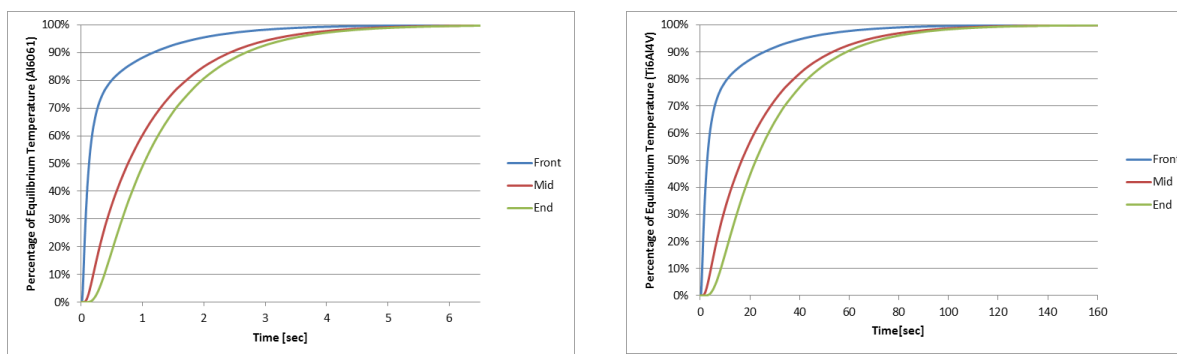


Fig. 7: Simulation of the time constant for the transducer made out of aluminum (Al6061, left) and titan (Ti6Al4V, right) respectively.

V. RADIATION EFFECTS IN OPTICAL FIBERS AND FBGS

The developed sensing elements shall open also the possibility to mount the sensors outside of the satellite where an extreme high total ionizing (TID) dose up to 25 Mrad or 250 kGy is expected. For this reason a detailed review of radiation effects in FBG sensors and in optical fibers is given.

A. Optical Fibers

Optical fibers have been widely used in space applications before, and many tests have been performed. Space flight qualification of optical fibers includes thermal and radiation tests, as well as mechanical tests like vibration and shock analyses. The highest impact on the fiber performance is the formation of color centers due to gamma-rays which increases the optical attenuation. The so-called radiation-induced attenuation (RIA), given in dB/km, indicates the radiation dependent loss per unit length. Henschel et al. [6] have shown that the fluor-doped fibers from Draka and Fujikura have the lowest loss (Fujikura 2 dB/km and Draka 10 dB/km after 10 Mrad (100 kGy)). By Aikawa et al. [1] it has been shown that an F-doped fiber has a very good recovery characteristic after irradiation. There are material compositions known which degrade the radiation hardness of a fiber, such materials are for example phosphor (P), nitrogen (N) and germanium (Ge). Phosphor has the highest impact; a fiber containing phosphor will see the highest radiation induced loss.

In the case here the maximum total ionizing dose is expected to be 25 Mrad (250 kGy) when the fiber is routed in or direct behind the satellite panels. During this development, two possible fiber types are evaluated in more detail. This are fluor (F) doped rad-hard fibers and pure silica fibers (SC-fiber). The F-doped fibers would be a good solution due to the high radiation resistance but writing FBGs into these kinds of fibers is challenging and no long-term stability of the gratings is guaranteed. This will be addressed in the next section.

B. Fiber-Bragg Gratings

Because of the possible use of FBG sensors in nuclear facilities many studies and tests have been carried out to observe the Bragg-wavelength shift (BWS) of FBGs during and after irradiation with gamma-rays [2]. By Grobnic et al. [3] it has been shown that FBGs written in F-doped fibers from Fujikura by the fs-IR technology have the lowest BWS of only 3–7 pm after 10 Mrad (100 kGy). No influence in BWS due to radiation was observed – either if the F-doped fiber was H₂-loaded or not. The results were identical for type I and type II gratings. For such gratings, the only existing drawback is the random long-term drift of the Bragg-wavelength which can be in the range of several pico-meters. It is assumed, that the fluor inside the fiber still reacts with other present materials which causes a small change in the relative refractive index change. The BWS in FBGs in standard fibers show a high impact to the H₂-loading before the writing process. For an unloaded standard single-mode telecommunication fiber (SMF28) a BWS of 10 pm after 100 kGy was observed, in contrast to 60 pm for the same hydrogen loaded fiber [3, 8]. The H₂-loading is necessary for standard fibers to enhance the photosensitivity to ultra-violet light which facilitates the grating inscription process. The pressure of the hydrogen loading has only small influence as shown by Henschel et al. [7].

If the FBGs are written in an N-doped fiber, the BWS shows no saturation at doses even higher than 1 MGy [4]. Such gratings are not suitable for temperature monitoring in space applications but could be used as radiation sensors inside satellites. Analysis of the BWS with different fiber coatings have been carried out by Gusarov et al. [5]. It has been shown therein, that the stripped fiber shows the lowest radiation sensitivity, whereas the Ormocer coated fiber shows the highest shift. This might be due the radiation induced altering effect in the

coating and the thereby created mechanical stress between fiber core and coating. The best behavior against radiation shows the polyimide coating.

To sum up, it can be said that gratings written by UV laser light in H₂-loaded fibers show the highest shift in wavelength. The effective change in Bragg-wavelength has its origin on the one hand in the refractive index change due to radiolytic rupture of the OH- and Ge-H bands inside the host material and on the other hand in an induced compacting which changes the grating pitch Λ . Nonetheless the H₂-loading before the writing process is indispensable to make the fiber photosensitive enough for an efficient writing of the gratings by UV laser light. By writing the gratings with an fs-IR laser light, the photosensitivity of the fiber is not relevant due the extreme high pulse energy which damages the fiber core locally (type II grating). The fs-IR written gratings show a much better performance due to radiation than the UV- and H₂-loaded type I gratings. But in contrast such grating are not stable over longer operating periods which is absolutely necessary for the project discussed here with a lifetime of 15 years. The idea in this study is to identify a pure silica fiber with the lowest radiation induced loss in which afterwards the FBGs are written by the fs-IR techniques. These gratings are then finally tested up to 25 Mrad and the shift in wavelength is observed.

VI. RADIATION TEST RESULTS

A. Standard UV-Written FBGs

The first step in the project was to use commercially available UV-written FBGs and to carry out a first gamma radiation test. For those gratings the standard writing process with hydrogen loading is applied. The commercial gratings which are used for testing had different packages, #101 and #103 had an SS304 steel tube with an outer diameter of 4.7 mm and 3.1 mm respectively, where #107 had no mechanical package around the FBG. For each type of grating three samples where tested. All test where carried out with a Co-60 source located at Fraunhofer INT institute.

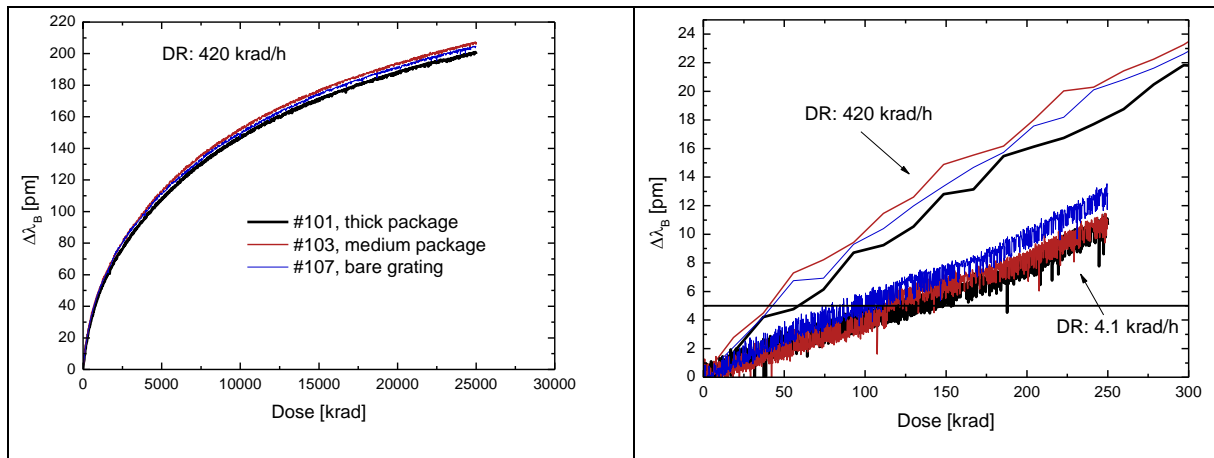


Fig. 8: High dose rate (left) and low dose rate (right) TID test of commercial UV-written gratings for different packages.

The radiation test results given in Fig. 8 indicate that the degradation of the tested sensors is too high to use the sensors for the planned activity. The assumed TID of 25 Mrad behind the satellite’s panels would result in a shift of Bragg-wavelength of approximately 200 pm which corresponds to a temperature error of 20°C. It has also been shown that the packaging of the sensor (bare fiber, 3 mm thick stainless steel tube, 5 mm thick stainless steel tube) has no effect on the induced wavelength shift. It is interesting that the FBGs irradiated with a lower dose rate (4.1 krad/h) have shown a shift of app. 10 pm after 250 krad whereas the tested FBGs with a higher dose rate (420 krad/h) have shown a shift of approximately 20 pm for the same TID. So a dose rate dependent effect was observed.

B. Pure Silica Optical Fibers

As mentioned before pure silica based fibers would also be good candidates for the planned application. So first of all, the radiation performance of the fiber must be evaluated. For this four samples from different manufacturers where tested up to 20 Mrad (200 kGy, dose rate 0.8 Gy/s), the results are depicted in Fig. 9. Only one sample from one manufacturer showed a discrepancy to the other sample fibers, this type of fiber is excluded from the following grating inscription test and subsequent radiation test. Values of 30 dB/km seem very high but two facts must be considered. Firstly, the used length in the planned application is in the range of

<20 meters which would result in an attenuation lower than 1 dB. And secondly, the test carried out was a high dose rate test. For low dose rates as they are expected in the planned application, the attenuation would be lower.

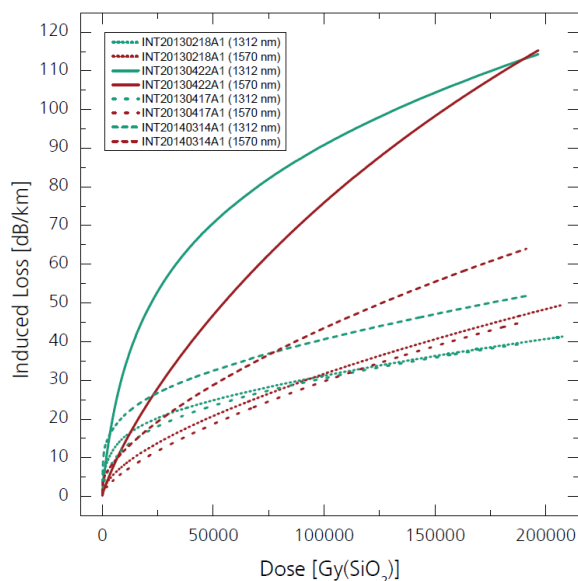


Fig. 9: Radiation test results of the pure silica fibers from four different manufacturers.

VII. FS-IR WRITTEN GRATINGS IN SELECTED FIBERS

After the two best samples with the lowest radiation-induced attenuation have been identified during the radiation test series, FBGs are written by the fs-IR technique. This step was necessary to prove if gratings can be written in this type of fibers. The gratings were written without any target specification just to test the writing process with this type of fiber. The writing is done by the Fraunhofer IOF institute in Jena by a special phase mask and a femto-second laser source. The test results are depicted in Fig. 10 for both fiber samples. The test has shown that it was possible to write the gratings into the selected fibers with a good spectral quality (especially for the spectrum shown on the left side), a high reflectivity of about more than 50 % and a flat transmission spectrum for light not corresponding to the Bragg-wavelength. This is very important when building WDM sensing systems with this kind of gratings. Again, it has to be noted that the gratings were written without a target specification to prove the concept.

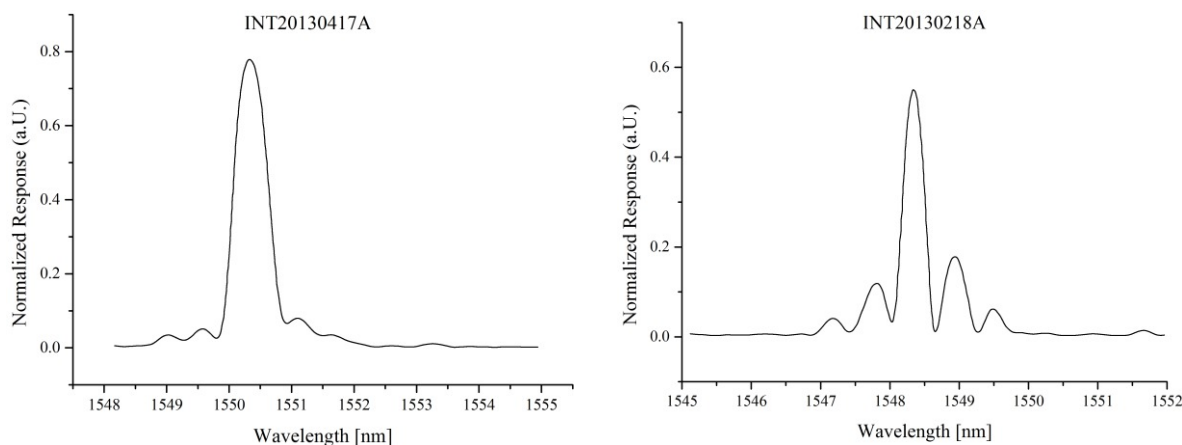


Fig. 10: Reflection spectra of FBGs written by fs-IR technique into two sample fibers.

VIII. FURTHER APPLICATIONS

Once a fiber and a FBG writing technique has been selected which sustains the radiation loads, the first step towards photonically-wired panels for satellites is done. One might think about combining sensing fibers embedded into the satellite panels with data transmission functionality with data rates in the GBit/s range. So

the fibers on the outside of the satellite build a neural system, which is able to sense physical parameters and can transport information as well.

IX. OUTLOOK

The next step is to establish a target specification for writing the sensors in the selected fibers. In addition the polarization dependency of the test gratings will be measured, this impacts the interrogator design. Also the writing of FBGs with different wavelength must be investigated under an economic point of view. One multiple samples of FBGs are written, a second radiation test will be carried out to identify the by radiation induced Bragg-wavelength shift. After this test it can be decided if the gratings can be used in the target application.

X. ACKNOWLEDGEMENT

The development of the FBG sensor was carried out within the “Hybrid Sensor Bus” project funded by ESA (4000104262/11/NL/US) and OHB System AG (formerly Kayser-Threde). We would specially thank to S. Nolte and C. Voigtländer from Fraunhofer IOF institute for writing the first two test gratings and J. Kuhnenn and S. Höffgen from Fraunhofer INT institute for the open and productive discussions concerning radiation issues and fiber selections.

XI. REFERENCES

- [1] K. Aikawa, K. Izoé, N. Shamoto, M. Kudoh, and T. Tsumanuma. Radiation-resistant single-mode optical fiber. *Fujikura Technical Review*, 37:9, 2008.
- [2] A. F. Fernandez, B. Brichard, and F. Berghmans. Long-term radiation effects on fiber Bragg grating temperature sensors in mixed gamma neutron fields. In *RADECS*, 2003.
- [3] D. Grobnic, H. Henschel, S. K. Hoeffgen, J. Kuhnenn, S. J. Mihailov, and U. Weinland. Radiation sensitivity of Bragg gratings written with femtosecond IR lasers. *SPIE-Fiber Optic Sensors and Applications VI*, 7316, 2009.
- [4] A. I. Gusarov, F. Berghmans, A. F. Fernandez, O. Deparis, Y. Defosse, D. Starodubov, M. Decreton, P. Megret, and M. Blondel. Behavior of fiber Bragg gratings under high total dose gamma radiation. *IEEE Transactions on Nuclear Science*, 47, No. 3:688, 2000.
- [5] A. I. Gusarov, C. Chojetzki, I. McKenzie, H. Thienpont, and F. Berghmans. Effect of the fiber coating on the radiation sensitivity of type I FBGs. *IEEE Photonics Technology Letters*, 20, No. 21:1802, 2008.
- [6] H. Henschel, D. Grobnic, S. K. Hoeffgen, J. Kuhnenn, S. J. Mihailov, and U. Weinand. Development of highly radiation resistant fiber Bragg gratings. *IEEE Transactions on Nuclear Science*, 58, No. 4:2103, 2011.
- [7] H. Henschel, S. K. Hoeffgen, J. Kuhnenn, and U. Weinand. Influence of manufacturing parameters and temperature on the radiation sensitivity of fiber Bragg gratings. *IEEE Transactions on Nuclear Science*, 57, No.4:2029, 2010.
- [8] H. Henschel, S.K. Hoeffgen, K. Krebber, J. Kuhnenn, and U. Weinand. Comparison of the radiation sensitivity of fiber Bragg gratings made by four different manufacturer. *IEEE Transactions on Nuclear Science*, 58, No. 3:906, 2011.
- [9] S. J. Mihailov, C. W. Semsler, D. Grobnic, R. B. Walker, P. Lu, H. Ding, and J. Unruh. Bragg gratings written in all-SiO₂ and Ge-doped core fibers with 800-nm femtosecond radiation and a phase mask. *Journal of Lightwave Technology*, 22, No. 1:94, 2004.
- [10] A. Othonos and Kalli K. *Fiber Bragg Gratings*. Artech House, 1999.
- [11] A. Othonos and X. Lee. Novel and improved methods of writing Bragg gratings with phase masks. *IEEE Photonic Technology Letters*, 7, No. 10:1183, 1995.
- [12] C. W. Semsler, S. J. Mihailov, and D. Grobnic. Formation of type I-IR and type II-IR gratings with an ultrafast IR laser and a phase mask. *Optics Express*, 13, No. 14:5377, 2005.